Supplement of Biogeosciences, 21, 4723–4737, 2024
https://doi.org/10.5194/bg-21-4723-2024-supplement

Biogeosciences
Open Access

Supplement of

Carbon degradation and mobilisation potentials of thawing permafrost peatlands in northern Norway inferred from laboratory incubations

Sigrid Trier Kjær et al.

Correspondence to: Sigrid Trier Kjær (sigrid.trier.kjar@nmbu.no)

Table S1: Operational layers in the three peat profiles. The deepest layers (PF3) at Áidejávri and Lakselv (indicated with *) were categorised as mineral soil based on visual inspection and chemical analysis.

Layer	Iškoras		Áidejávri		Lakselv	
	Top (cm)	Bottom (cm)	Top (cm)	Bottom (cm)	Top (cm)	Bottom (cm)
AL1	0	15	0	15	2	12
AL2	25	35	20	35	20	35
AL3	45	55	40	50	40	60
TZ	60	73	50	60	60	70
PF1	80	86	69	80	70	80
PF2	106	118	89	100	80	85
PF3	150	162	104*	110*	85*	95*

Table S2: Operational layers in the thermokarst peat profile.

Layer	Iškoras		Áidejávri	
	Top (cm)	Bottom (cm)	Top (cm)	Bottom (cm)
New peat	N/A	N/A	0	10
Old active layer	10	20	20	30
Top old permafrost	40	46	60	65
Bottom old permafrost	80	92	90	95

Table S3: Comparison of CO_2 accumulation (96 days) in loose oxic incubations of permafrost and thermokarst core samples from Áidejávri and Iškoras. The different layers of the thermokarst core are compared to corresponding layers in the permafrost core (AL1, PF1 and PF2/PF3) as shown in Fig 1. PF2 was used as the deep permafrost sample at Áidejávri because of mineral soil in PF3. For absolute depths, see tables S1 and S2.

µmol CO_2 g dw^{-1} 96 $days^{-1}$					
Permafrost core			Thermokarst core		
	Iškoras	Áidejávri		Iškoras	Áidejávri
			New peat		616
AL1	411	250	TK-AL	177	241
PF1	173	255	TK-PF1	40	62
PF2/PF3	97	101	TK-PF2/3	92	85

Table S4: Comparison of cumulative CH_4 production (96 days) in loose anoxic incubations of permafrost core and thermokarst core samples at Áidejávri and Iškoras. The different layers of the thermokarst core are compared to corresponding layers in the permafrost core (AL1, PF1 and PF2/PF3) as shown in Fig 1. PF2 was used as the deep permafrost sample at Áidejávri because of mineral soil in PF3. For absolute depths, see tables S1 and S2.

nmol CH_4 g dw^{-1} 96 $days^{-1}$					
Permafrost core			Thermokarst core		
	Iškoras	Áidejávri		Iškoras	Áidejávri
			New peat		335
AL1	3	3	TK-AL	19661	7014
PF1	44	159	TK-PF1	1824	77
PF2/PF3	5	49	TK-PF2/3	3127	262

Table S5: Geochemical properties of thermokarst samples at the beginning of incubation.

	Iškoras		Áidejávri	
	pH	DOC mg g dw^{-1}	pH	DOC mg g dw^{-1}
New peat			3.62 ± 0.05	2.29 ± 0.21
TK-AL	3.3 ± 0.02	1.01 ± 0.09	3.40 ± 0.09	2.03 ± 0.57
TK-PF1	3.44 ± 0.05	1.14 ± 0.02	4.25 ± 0	0.66 ± 0.01
TK-PF2/3	3.84 ± 0.005	1.85 ± 0.06	5.11 ± 0.01	0.83 ± 0.03

Table S6: Average (n=4) CO_2 and CH_4 accumulation (±SD) of TZ and PF samples during over-night thawing. Bottles were flushed with He before thawing to ensure anoxic conditions and equal gaseous concentrations. No data are available for Lakselv due to technical reasons.

Layers	Iškoras		Áidejávri	
	µmol CO_2 g dw^{-1}	nmol CH_4 g dw^{-1}	µmol CO_2 g dw^{-1}	nmol CH_4 g dw^{-1}
TZ	4.5 ± 0.9	171 ± 49	2.1 ± 0.1	9 ± 3
PF1	3.3 ± 0.2	128 ± 19	2 ± 0.2	44 ± 4
PF2	3 ± 0.5	170 ± 59	1.5 ± 0.1	71 ± 8
PF3	2.1 ± 0.1	144 ± 9	0.3 ± 0.01	8 ± 1

Table S7: Comparison of CO_2 and CH_4 production potentials in this study with Kirkwood et al. (2021). Average cumulative anoxic CO_2 production was 2014 and 1282 µg CO_2 g dw^{-1} 225 d^{-1} in active layer and permafrost, respectively and average cumulative anoxic CH_4 production was 215 and 611 µg CH g dw^{-1} 225 d^{-1} in active layer and permafrost, respectively (Kirkwood, 2021). Cumulative CO_2 and CH_4 production in loosely packed samples from this study were adjusted to 14°C using Q10 =2 and reported as µg g dw^{-1} 225 d^{-1}. *PF3 was mineral soil and not included in the average for Áidejávri and Lakselv.

Layer	Iškoras		Áidejávri		Lakselv	
	µg CO_2 g^{-1} 225 d^{-1}	µg CH_4 g^{-1} 225 d^{-1}	µg CO_2 g^{-1} 225 d^{-1}	µg CH_4 g^{-1} 225 d^{-1}	µg CO_2 g^{-1} 225 d^{-1}	µg CH_4 g^{-1} 225 d^{-1}
AL1	9627.4	107.7	5992.3	83.7	3758.2	53.7
AL2	2430.4	19.1	5868.3	2.2	1497.3	6.9
AL3	2202.2	4.0	2559.3	5.8	2798.9	30.5
TZ	4092.8	2241.6	5091.6	111.1	2497.3	42.0
PF1	3452.6	1100.5	2513.3	18988.8	1398.3	7562.4
PF2	2074.0	116.3	4754.2	1204.1	660.9	19426.4
PF3	2478.4	649.0	783.2	2826.6	368.2	599.2
Average AL	4753.3	43.6	4806.6	30.5	2684.8	30.4
Average PF*	3024.5	1026.8	4119.7	6768.0	1518.8	9010.2

Table S8: Comparison of CO_2 production potentials with Treat et al. (2014). The cumulative CO2 production reported by Treat et al. (2014) for the Alaskan peat plateau were roughly 4 and 2 mg CO_2-C g C^{-1} 30 d^{-1} for oxic and anoxic incubation, respectively. Cumulative CO_2 production from loosely packed samples in this study was adjusted to 20°C using Q10 =2 and reported in mg CO_2-C g C^{-1}.

	mg CO_2-C g C^{-1} 30 $days^{-1}$					
	Iškoras		Áidejávri		Lakselv	
Layer	Oxic	Anoxic	Oxic	Anoxic	Oxic	Anoxic
AL1	10.77	6.01	9.66	3.92	3.88	1.14
AL2	0.94	0.60	1.80	0.84	0.83	0.33
AL3	0.82	0.56	1.34	0.60	0.92	0.44
TZ	5.61	2.35	5.68	1.69	1.44	1.20
PF1	5.41	2.11	6.79	0.87	3.46	1.19
PF2	2.91	1.15	5.07	0.85	4.67	0.33
PF3	2.84	1.44	9.63	6.84	0.45	0.14

Table S9: Comparison of CO_2 production potentials with Waldrop et al. (2021). The incubations showed no difference in cumulative CO_2 production across horizons and CO_2 accumulation was therefore given as an average over the whole peat column. Measured average oxic respiration was 831 µmol CO_2 g C^{-1} 6 $months^{-1}$ and anoxic respiration 214 µmol CO_2 g C^{-1} 6 $months^{-1}$. Cumulative CO_2 production after 6 months (183 days) was calculated using interpolated values from long term incubation of loosely packed samples. Temperature was adjusted to 5°C using Q10 =2 and reported as µmol CO_2 g C^{-1} 6 $months^{-1}$.

	µmol CO_2 g C^{-1} 6 $months^{-1}$					
	Iškoras		Áidejávri		Lakselv	
Layer	Oxic	Anoxic	Oxic	Anoxic	Oxic	Anoxic
AL1	628.48	215.43	392.78	143.92	333.38	76.62
AL2	125.95	48.26	171.82	117.14	138.33	34.22
AL3	109.14	43.99	148.06	52.73	133.04	63.83
TZ	286.79	99.24	396.70	107.83	183.96	88.27
PF1	343.34	80.79	413.36	55.47	332.21	71.13
PF2	140.06	45.35	291.78	N/A	448.65	26.51
PF3	190.79	58.85	1001.08	327.86	49.27	12.70
Average	260.65	84.56	402.23	134.16	231.26	53.33

Table S10: pH measured in the beginning and the end of oxic and anoxic incubations.

	pH					
	Iškoras		Áidejávri		Lakselv	
Layer	0 days	358 days	0 days	363 days	0 days	354
Oxic incubation						
AL1	2.8	3.04	3.4	3.08	3.6	3.19
AL2	3.1	3.24	3.7	3.74	4.2	3.85
AL3	3.2	3.49	3.9	3.52	4.5	4.09
TZ	3.8	4.09	4.3	3.95	4.7	4.1
PF1	3.9	4.2	5.4	4.13	5.5	4.6
PF2	4.2	4.28	5.5	4.02	5.2	4.48
PF3	4.5	4.14	5.4	3.41	5.5	4.16
Anoxic incubation						
AL1	2.8	3.26	3.6	3.06	3.3	3.28
AL2	3.1	3.52	3.7	3.67	4.1	4.12
AL3	3.2	3.7	4.0	3.62	4.5	4.43
TZ	3.8	4.23	4.4	4.29	4.7	4.7
PF1	3.9	4.22	4.6	4.57	5.6	5.17
PF2	4.2	4.44	5.5	3.97	5.1	4.86
PF3	4.5	4.74	5.5	5.02	5.5	5.06

Table S11: Gravimetric water content (%)

	Iškoras	Áidejávri	Lakselv
Permafrost core			
AL1	782	391	334
AL2	479	258	277
AL3	450	492	304
TZ	740	1044	251
PF1	641	1250	401
PF2	624	720	479
PF3	760	70	67
Thermokarst core			
New peat		969	
TK-AL	543	642	
TK-PF1	448	335	
TK-PF2/3	786	517	

Table S12: Anoxic CO_2 production as percentage of oxic CO_2 production throughout 350 days.

Iškoras	Áidejávri	Lakselv
32.2	37.3	24.8
28.7	61.2	26.1
29.5	40.6	54.3
23.9	28.6	40.5
17.0	13.1	18.3
26.3	#N/A	6.8
25.1	29.9	21.7

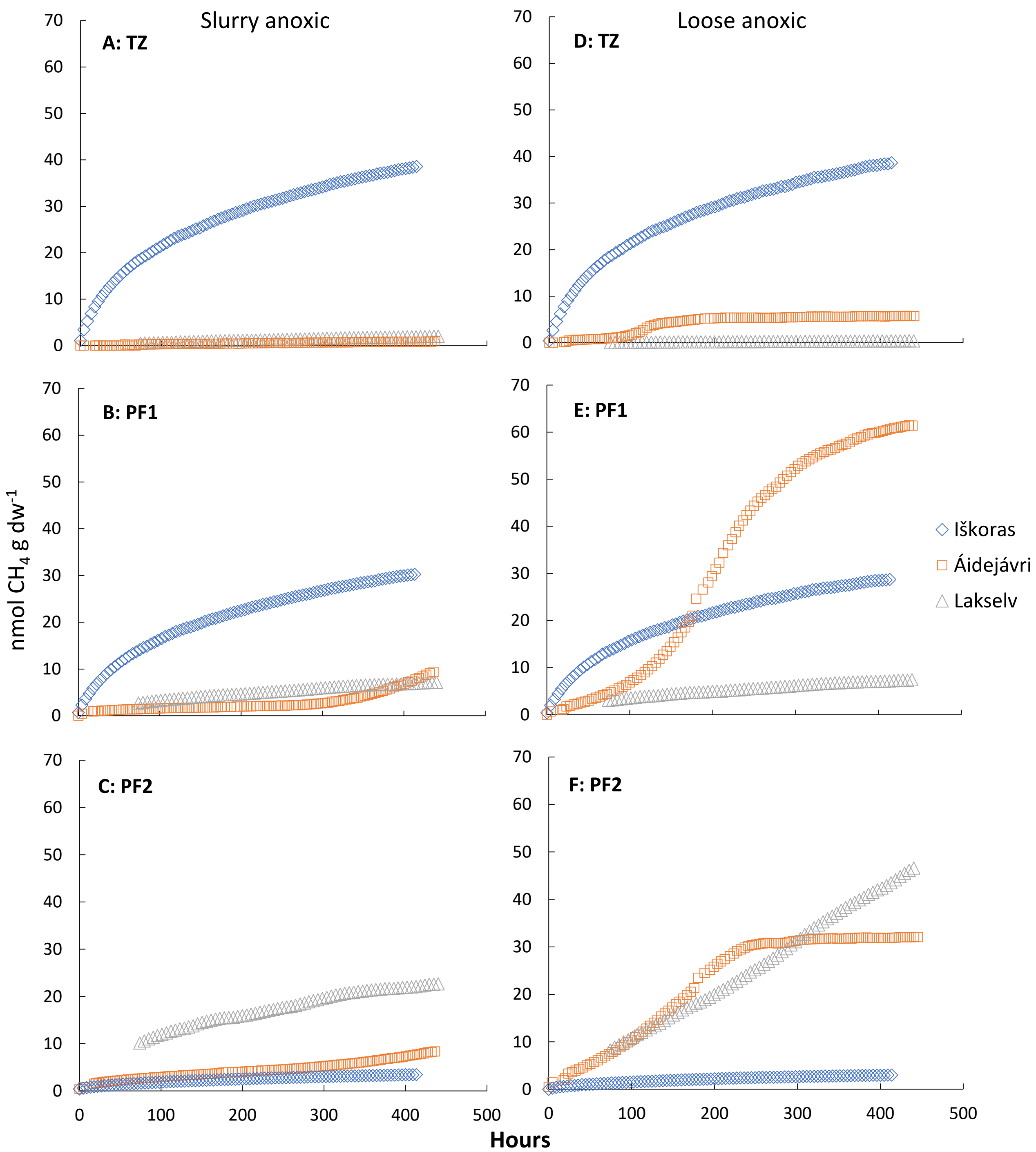

Figure S1: Comparison of CH_4 accumulation kinetics across peat plateaus (until day 19) for two treatments; left panel: slurry anoxic; right panel: loose anoxic, for samples from TZ, PF1, and PF2. A: Slurry anoxic TZ. B: Slurry anoxic PF1. C: Slurry anoxic PF2. D: Loose anoxic TZ. E: Loose anoxic PF1. F: Loose anoxic PF2

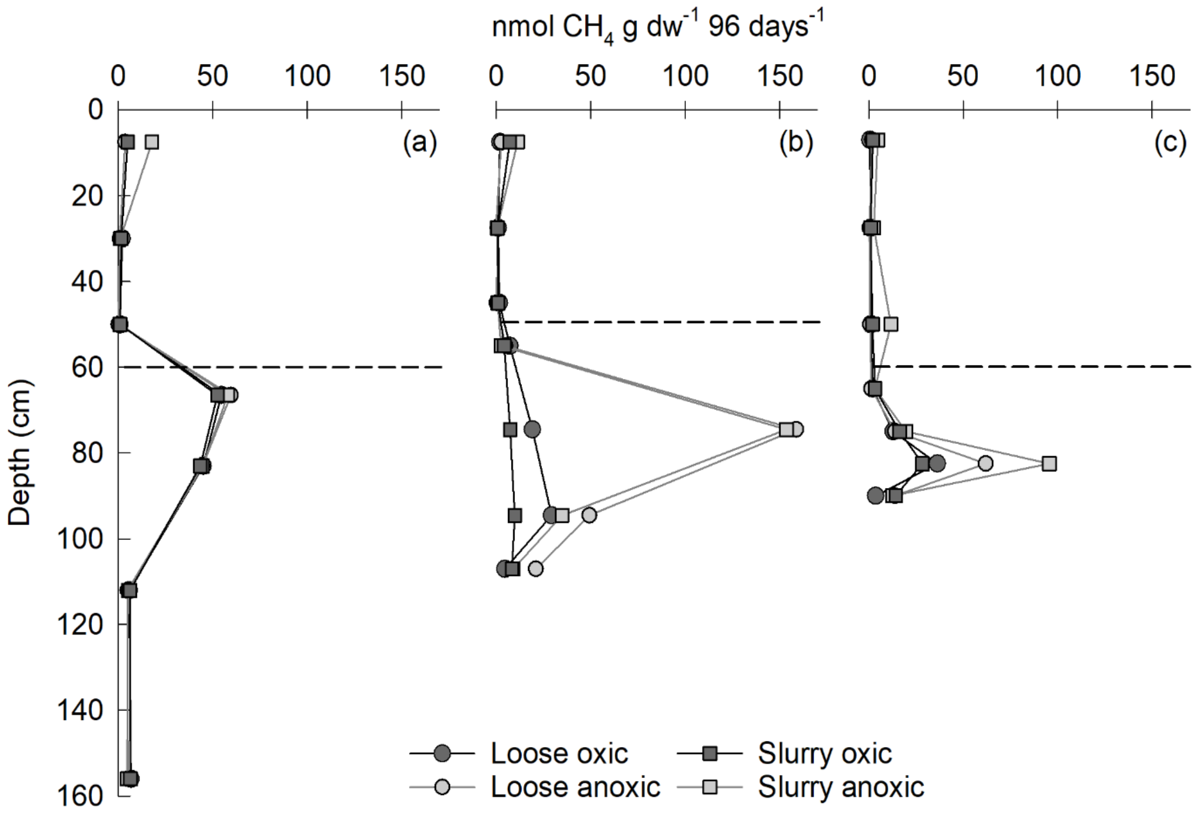

Figure S2: Cumulative CH_4 production (96 d) over depth under different incubation conditions (treatments). (a) Iškoras, (b) Áidejávri and (c) Lakselv. The depth is given as the average depth of the incubated sample. Stippled line indicates thaw depth at sampling time.

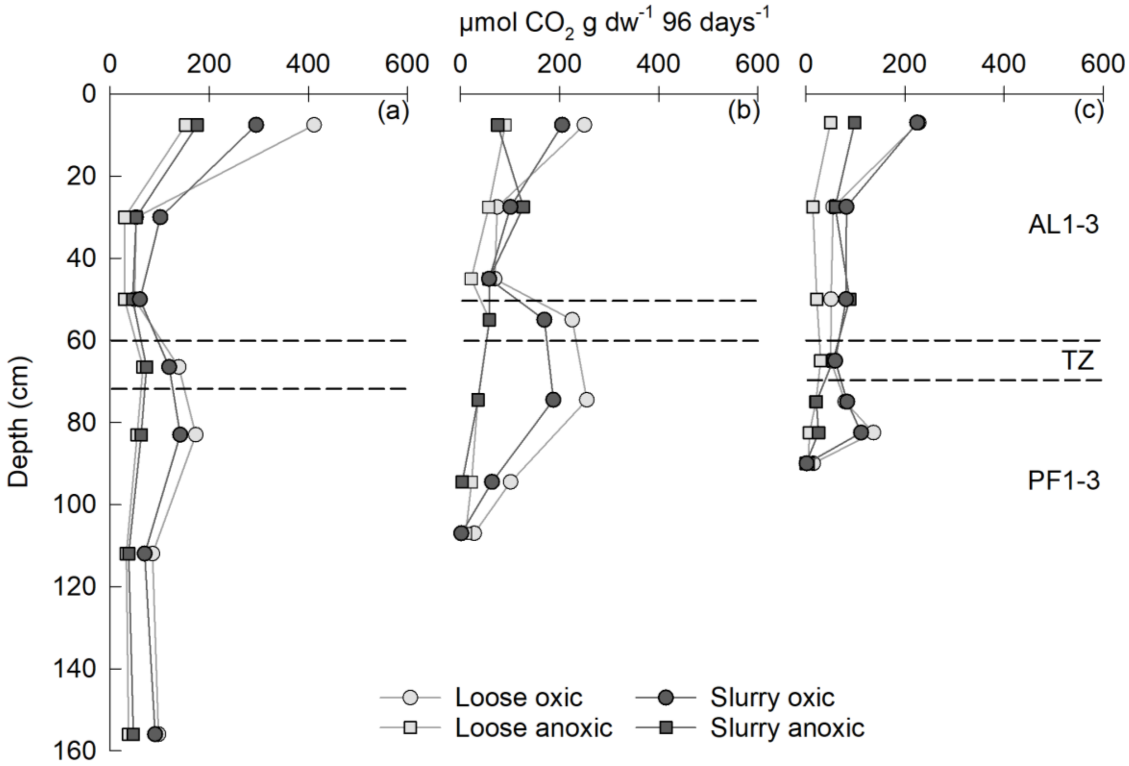

Figure S3: Cumulative CO_2 production (96 d) over depth and 96 days under different incubation conditions (treatments). (a) Iškoras, (b) Áidejávri and (c) Lakselv. The depth is given as the average depth of the incubated sample. Stippled line indicates thaw depth at sampling time.

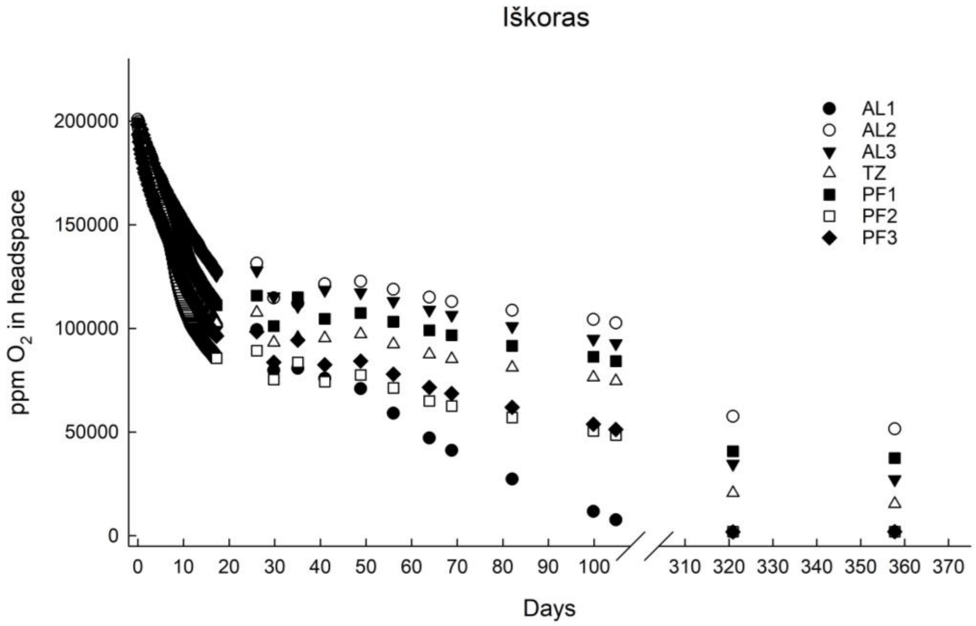

Figure S4: Kinetics of O_2 depletion in initially oxic incubations of loosely packed samples from Iškoras. Shown are measured headspace concentrations not corrected for dilution. The rapid decline during the first 17-19 days of incubation is due to dilution from He back-pumping.

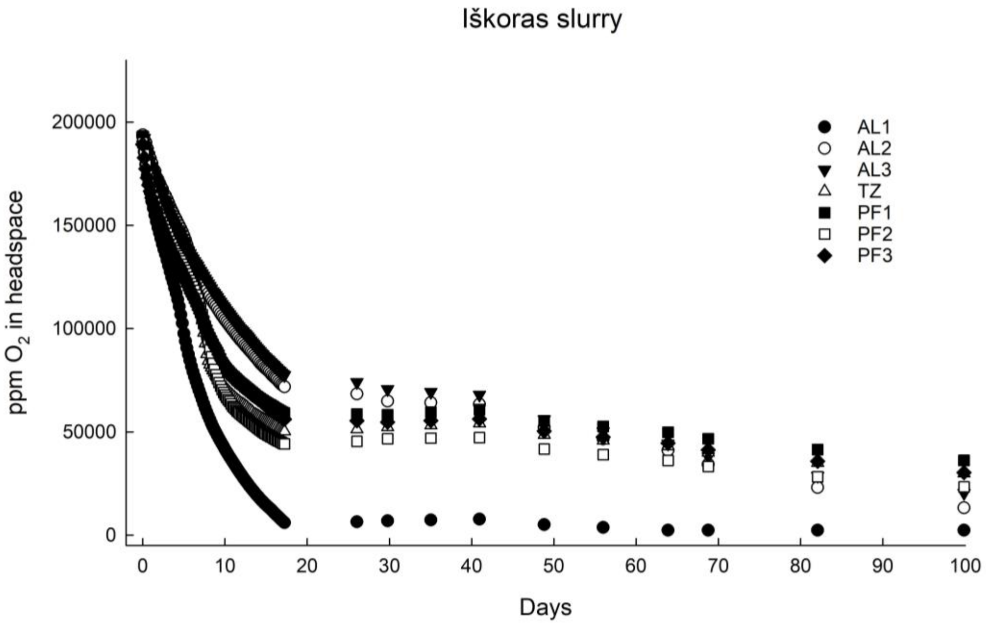

Figure S5: Kinetics of O_2 depletion in initially oxic incubations of slurry samples from Iškoras. Shown are measured headspace concentrations not corrected for dilution. The rapid decline during the first 17-19 days of incubation is due to dilution from He back-pumping.

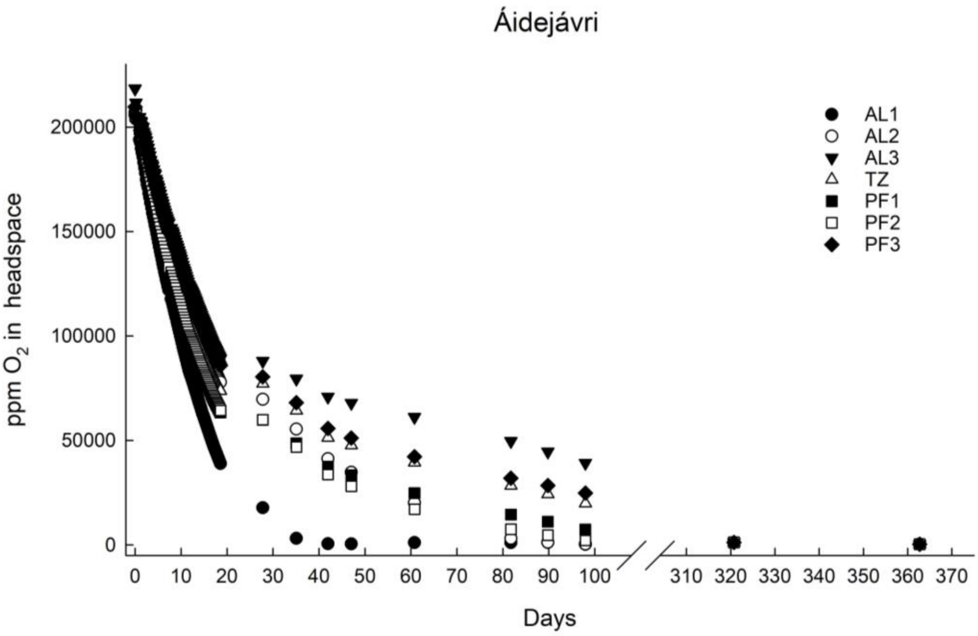

Figure S6: Kinetics of O_2 depletion in initially oxic incubations of loosely packed samples from Áidejávri. Shown are measured headspace concentrations not corrected for dilution. The rapid decline during the first 17-19 days of incubation is due to dilution from He back-pumping. PF2 had a leakage and could not be measured in the two last samplings.

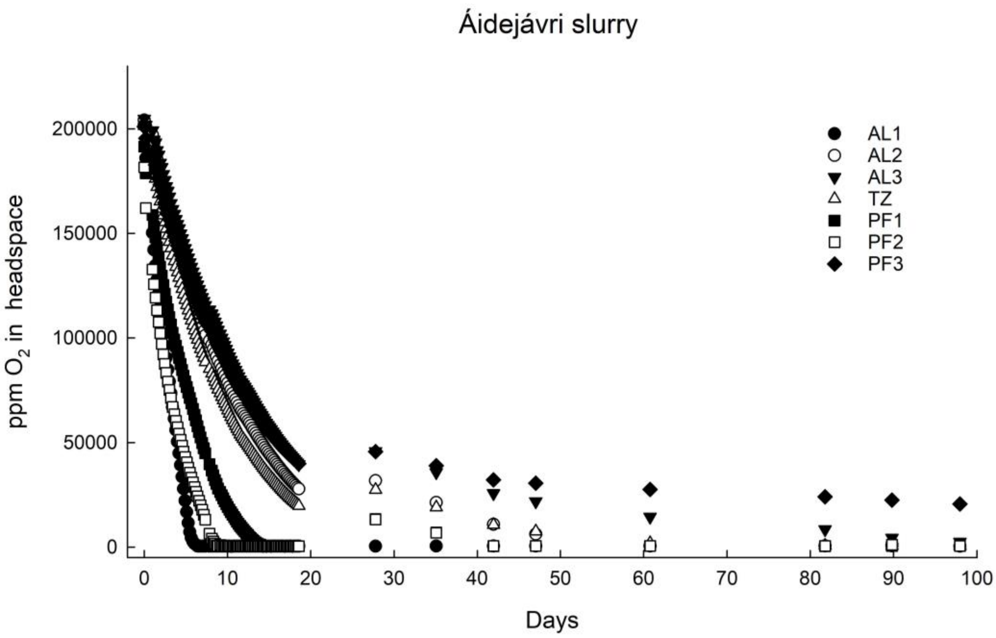

Figure S7: Kinetics of O_2 depletion in initially oxic incubations of slurry samples from Áidejávri. Shown are measured headspace concentrations not corrected for dilution. The rapid decline during the first 17-19 days of incubation is due to dilution from He back-pumping.

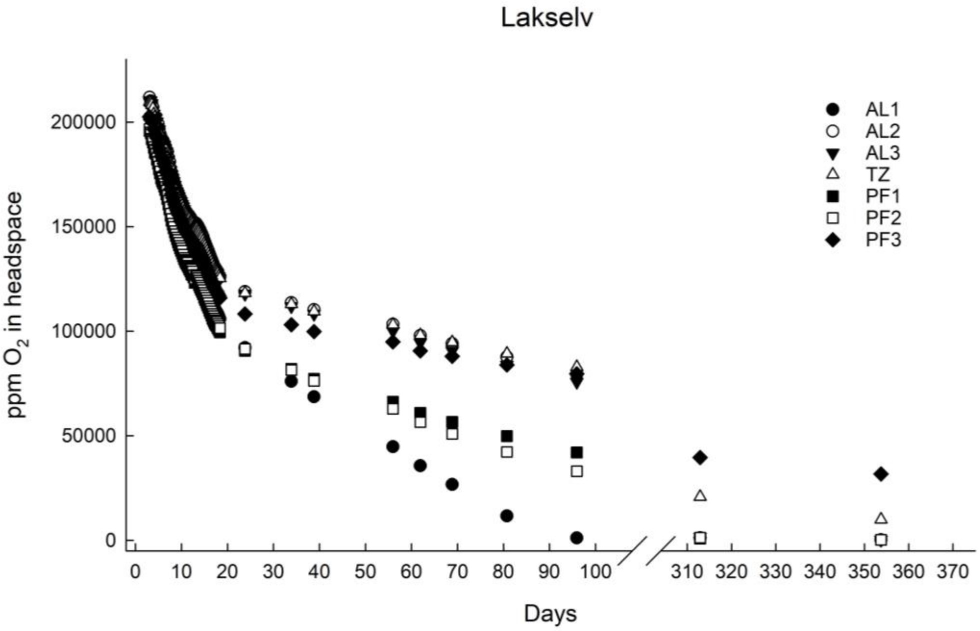

Figure S8: Kinetics of O_2 depletion in initially oxic incubations of loosely packed samples from Lakselv. Shown are measured headspace concentrations not corrected for dilution. The rapid decline during the first 17-19 days of incubation is due to dilution from He back-pumping.

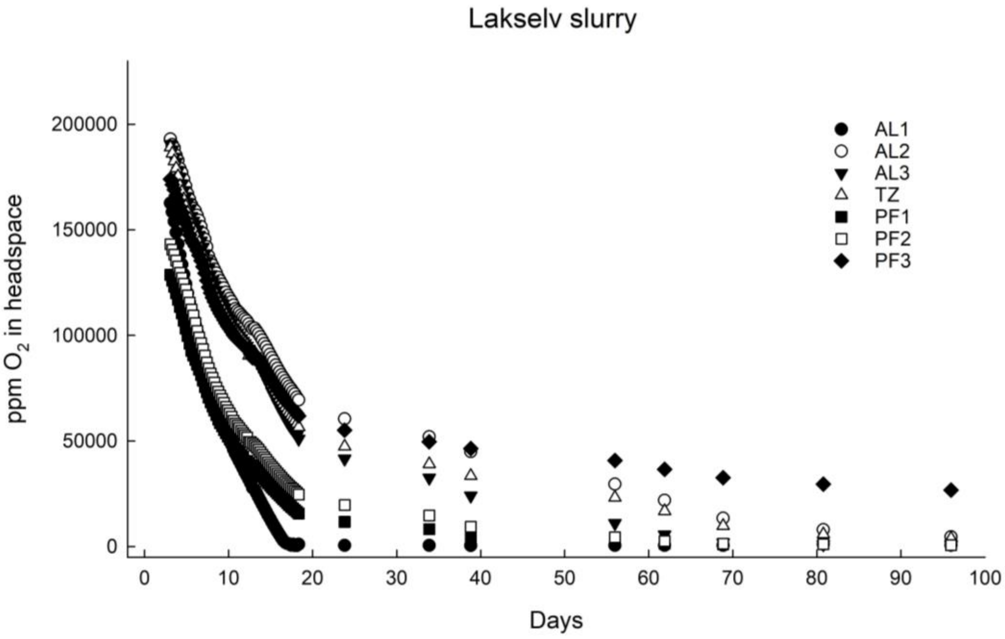

Figure S9: Kinetics of O_2 depletion in initially oxic incubations of slurry samples from Lakselv. Shown are measured headspace concentrations not corrected for dilution. The rapid decline during the first 17-19 days of incubation is due to dilution from He back-pumping.

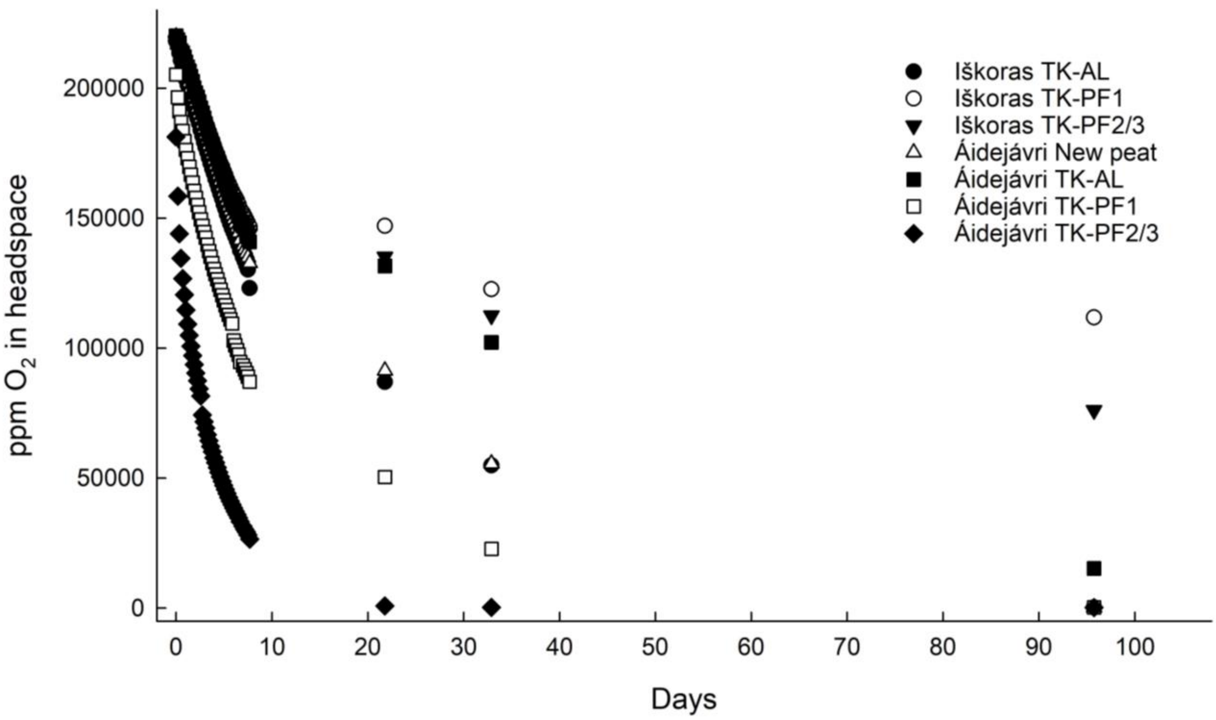

Figure S10: Kinetics of O_2 depletion in initially oxic incubations of loosely packed samples from thermokarst cores from Iškoras and Áidejávri. Shown are measured headspace concentrations not corrected for dilution. The rapid decline during the first 9 days of incubation is due to dilution from He back-pumping.

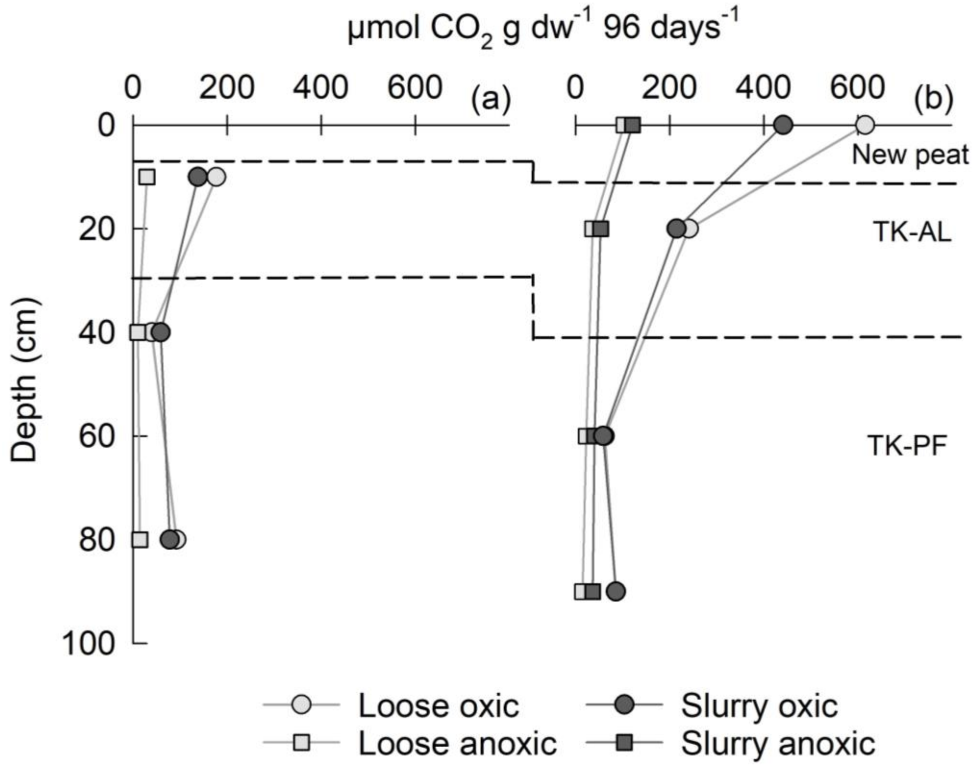

Figure S11: Cumulative CO_2 production (96 d) over depth in thermokarst cores under different incubation conditions (treatments). (a) Iškoras and (b) Áidejávri. Stippled line indicates different layers in the thermokarst core.

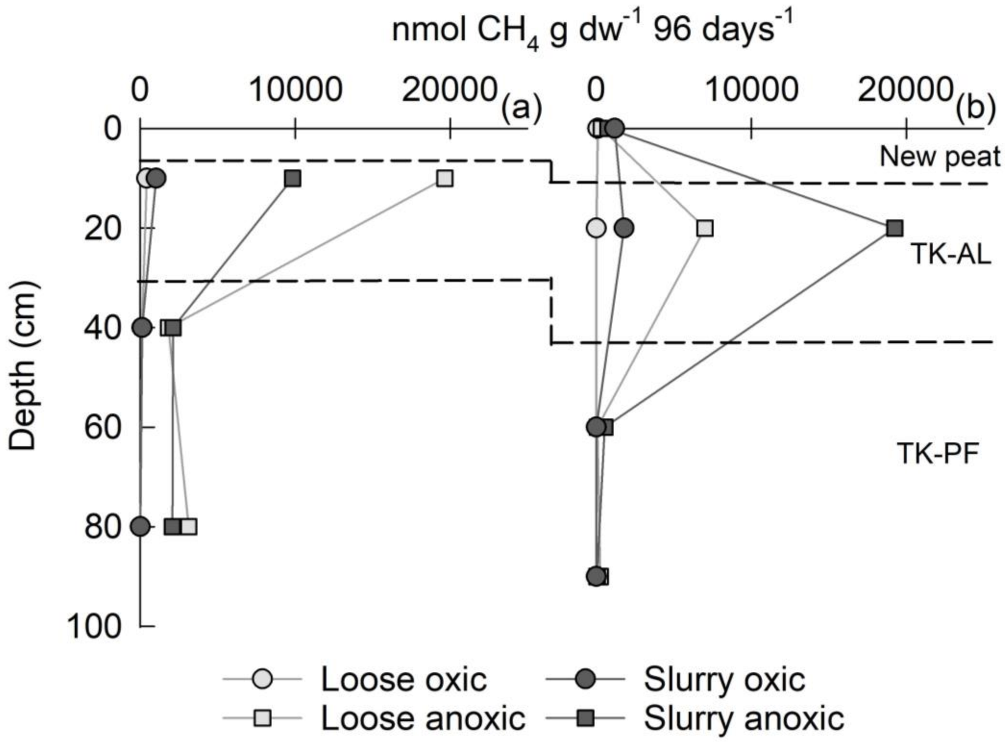

Figure S12: Cumulative CH_4 production (96 d) over depth in thermokarst cores under different incubation conditions (treatments). (a) Iškoras and (b) Áidejávri. Stippled line indicates different layers in the thermokarst core.

References

Kirkwood, A.: Kirkwood_GBC_Supp-Info_Data.xlsx, 10.6084/m9.figshare.14546823.v1, 2021.

Kirkwood, J. A. H., Roy-Léveillée, P., Mykytczuk, N., Packalen, M., McLaughlin, J., Laframboise, A., and Basiliko, N.: Soil Microbial Community Response to Permafrost Degradation in Palsa Fields of the Hudson Bay Lowlands: Implications for Greenhouse Gas Production in a Warming Climate, Global Biogeochemical Cycles, 35, e2021GB006954, https://doi.org/10.1029/2021GB006954, 2021.

Kjær, S. T.: Constraints for carbon degradation in subarctic thawing peatland permafrost in Northern Scandinavia, MSc thesis, Norwegian University of Life Sciences, https://hdl.handle.net/11250/2788732, 2021

Treat, C. C., Wollheim, W. M., Varner, R. K., Grandy, A. S., Talbot, J., and Frolking, S.: Temperature and peat type control CO_2 and CH_4 production in Alaskan permafrost peats, Global Change Biology, 20, 2674-2686, https://doi.org/10.1111/gcb.12572, 2014.

Waldrop, M. P., McFarland, J., Manies, K. L., Leewis, M. C., Blazewicz, S. J., Jones, M. C., Neumann, R. B., Keller, J. K., Cohen, L., Euskirchen, E. S., Edgar, C., Turetsky, M. R., and Cable, W. L.: Carbon Fluxes and Microbial Activities From Boreal Peatlands Experiencing Permafrost Thaw, J Geophys Res-Biogeo, 126, e2020JG005869, https://doi.org/10.1029/2020JG005869, 2021.